Self-organizing super-structures formed from hydrogen-bonded biimidazolate metal complexes

Makoto Tadokoro*†, Hideaki Kanno‡, Tadanori Kitajima*, Hiromi Shimada-Umemoto*, Noritaka Nakanishi*, Kiyoshi Isobe§, and Kazuhiro Nakasuji¶

*Department of Chemistry and §Department of Material Science, Graduate School of Science, Osaka City University, Sumiyoshi-ku, Osaka 558-8585; ‡Department of Chemistry, Faculty of Science, Shizuoka University, Otani 836, Shizuoka 422-8529; and ¶Department of Chemistry, Graduate School of Science, Osaka University, Toyonaka, Osaka 560-0043, Japan

Edited by Jack Halpern, University of Chicago, Chicago, IL, and approved January 30, 2002 (received for review December 11, 2001)

Manipulation of molecular crystals formed from self-organization is one of the important methods to develop the new molecular functional materials. In particular, we look upon mutual cohesive interactions of hydrogen bonding and metal coordination as one useful tool to construct the preprogramming superstructures. In this study, five controlled superstructures of a one-dimensional linear chain—a zigzag ribbon, right-handed and left-handed helices, and a two-dimensional honeycomb sheet—-are newly created by using the neutral metal complexes with some 2,2′-biimidazolate mono-anions.

Molecular arrays with desirable topological networks recently have been realized in crystal by self-organized binding between molecular building blocks with hydrogen-bonding (H-bonding) and metal-coordinating affinities. The coordination bonds and the H-bonds are relatively weak interactions that impart strength, directionality, and complementarity (1–6). Such crystal manipulations, often known through crystal engineering, are performed to yield arrays of controlled superstructures that provide new functional molecular solids (7–8). Thus, the self-organization of designed molecules containing certain kinds of complementary H-bonding and coordinating units has stimulated new efforts in the material sciences that use, for example, controlled molecular arrays adsorbed to a solid surface (9–11), a self-organized molecular assembly with unique cavities (12), and an integrated system of molecular device (13).

In some molecular systems, it has been possible to control molecular aggregation in the crystal by the difunctional ligands that bond to metal with coordinate–covalent interactions and to each other with H-bonding interactions (14–19). The 2,2′-biimidazolate mono-anion ($Hbim^{-1}$), recently introduced (20), works as such a difunctional bridging ligand not only to form a stable metal-chelate complex but also a new intermolecular complementary H-bonding with two sets of NH donors and N acceptors, as shown in Scheme 1. A molecular system like

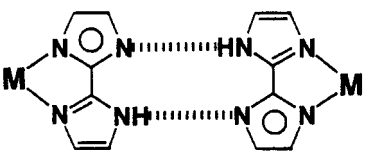

1

Scheme 1

$Hbim^{-1}$ has not been found in molecular aggregation used for crystal engineering except in our aggregation system.

The previously reported $[Ni^{II}(Hbim)_3]^{-1}$, obtained by self-organization with an Ni(II) ion and an $Hbim^{-1}$, forms a variety of multidimensional superstructures with long-range ordered arrays (21). In these cases, the nature of the metal anion assembly was affected by the nature and size of the counter cation. We have tried to eliminate the counter ion and to create a new superstructure with an infinite chain without the effect of counter ions on the assembly of metal complexes constructed from the H-bonding dimer units like Scheme 1. In this report, four types of self-organizing superstructures with infinite chains are identified by designing four neutral $Hbim^{-1}$ complexes with altered metal coordination spheres. As the result, we can systematically produce five types of preprogramming superstructures (shown in Fig. 1) of a dimer (*A*), a linear chain (*B*), a zigzag ribbon (*C*), a honeycomb sheet (*D*), and a helical chain (*E*), respectively (see data sheets, which are published as supporting information on the PNAS web site, www.pnas.org).

Materials and Methods

Preparation of *trans*-$[Ni^{II}(Hbim)_2(^tBupy)_2]$ (Complex 2). H_2bim (0.40 g, 3 mmol) and 4-*tert*-butyl pyridine (^{t}Bupy) (0.28 g, 2.0 mmol) were added to MeOH (60 cm^3) containing potassium *tert*-butoxide (1.10 g, 10 mmol), and the suspension was heated until the refluxing condition was achieved. To the resulting solution, $Ni(ClO)_4{\cdot}6H_2O$ (0.36 g, 1.0 mmol) in MeOH (40 cm^3) was added dropwise. The reaction mixture was refluxed for 15 min and filtered. The obtained filtrate was cooled slowly to room temperature and left overnight. The orange-prism crystals were obtained after several days. Elemental analysis was as follows: for $[Ni(Hbim)_2(^tBupy)_2]{\cdot}0.5H_2O$ ($C_{30}H_{37}N_{10}O_{0.5}Ni$), calculated values were C, 59.62%; H, 6.17%; N, 23.18%: values found were C, 59.40%; H, 5.98%; N, 23.39%; (the sample was dried under vacuum for 6 h at 100°C), IR (KBr) 2656 cm^{-1}[*br*, ν (NH)]; 1910 cm^{-1} [*br*, 2γ (NH)].

Preparation of $[Ni^{II}(Hbim)_2(bpy)]$ (Complex 3). The blue crystals of complex **3** were obtained in a similar way to that of the crystals of complex **2**, except for using 2,2′-bipyridine (bpy) (0.16 g, 1.0 mmol) instead of ^{t}Bupy. Elemental analysis: for $[Ni(Hbim)_2(bpy)]$ ($C_{22}H_{18}N_{10}Ni$), calculated values were C, 54.91%; H, 3.77%; N, 29.11%: values found were C, 54.56%; H, 3.88%; N, 28.79%; (the sample was dried under vacuum for 6 h at 100°C), IR (KBr) 2788 cm^{-1}[*br*, ν (NH)]; 1919 cm^{-1} [*br*, 2γ (NH)].

Preparation of $[Ru(Hbim)_3]$ (Complex 4). Synthesis of the crystals of complex **4** was performed as described (22). Elemental analysis:

This paper was submitted directly (Track II) to the PNAS office.

Abbreviations: ^{t}Bupy, 4-*tert*-butyl pyridine; bpy, 2,2′-bipyridine; 1-D, one-dimensional.

Data deposition: The atomic coordinates have been deposited in the Cambridge Structural Database, Cambridge Crystallographic Data Centre, Cambridge CB2 1EZ, United Kingdom [CSD reference nos. 174718 (**2**), 174719 (**3**), 174720 (**4**), 174721 (**5**), and 174927 (**6**)].

†To whom reprint requests should be addressed. E-mail: tadokoro@sci.osaka-cu.ac.jp.

www.pnas.org/cgi/doi/10.1073/pnas.072661699

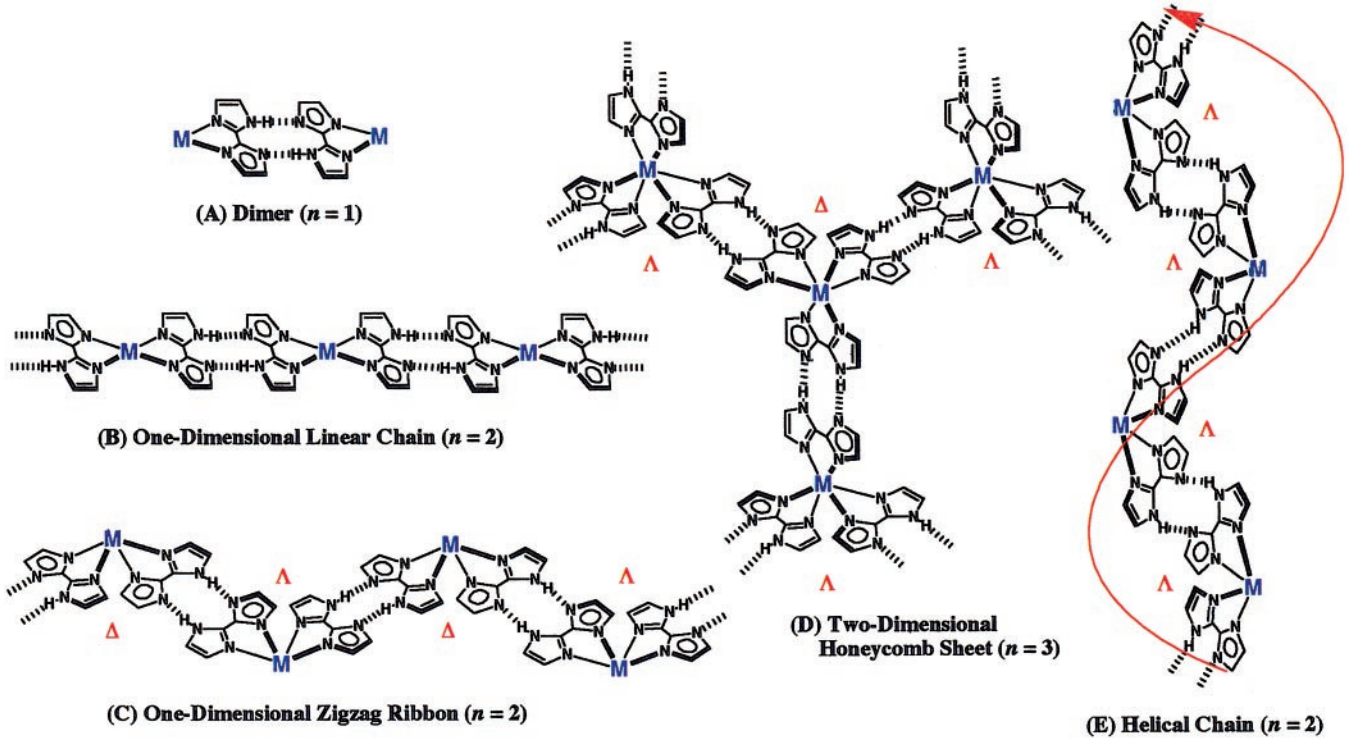

Fig. 1. Schematic representations of multidimensional assemblies formed by transition-metal complexes with controlled configurations that regulate the number of $Hbim^{-1}$ ligands. (*A*) ''Zero-dimensional dimer'' constructed by the complementary intermolecular hydrogen bonds between $Hbim^{-1}$ ligands in the metal complexes coordinated by only one $Hbim^{-1}$ ligand. (*B*) One-dimensional linear chain assembled by the metal complexes with *trans*-configuration coordinated by two $Hbim^{-1}$ ligands. (*C*) One-dimensional zigzag ribbon assembled by the metal complexes with at least two $Hbim^{-1}$ ligands in *cis*-configuration. (*D*) Two-dimensional honeycomb sheet linked by three intermolecular hydrogen bondings of the metal complexes with three $Hbim^{-1}$ ligands. The sheet is constructed by hydrogen bondings with alternate linkage between different optical isomers of Δ and λ types. (*E*) Helical chain assembled by intermolecular hydrogen bondings between the same optical isomers of Δ or λ containing at least two $Hbim^{-1}$ ligands. *n* = number of $Hbim^{-1}$ ligands coordinated to transition metal ions.

for $[Ru(Hbim)_3]\cdot 1/2H_2O$ ($C_{18}H_{16}N_{12}O_{0.5}Ru$), calculated values were C, 42.44%; H, 3.17%; N, 32.99%; values found were C, 42.77%; H, 3.29%; N, 32.61%; (the sample was dried under vacuum for 6 h at 100°C), IR (KBr) 2502 cm^{-1} [*br*, ν (NH)]; 1890 cm^{-1} [*br*, 2γ (NH)].

Preparations of Δ-[$Co^{III}(Hbim)_3$] (Complex 5) or λ-[$Co^{III}(Hbim)_3$] (Complex 6). A methanol solution of sodium methoxide (28%) was added to a methanolic suspension (5 cm^3) of the optically resolved cobalt (III) complex of Δ− or λ-$[Co^{III}(Hbim)_3](NO_3)_3$ (0.10 g, 0.15 mmol) until the mixture became an orange solution. The cobalt (III) complex was resolved according to the method described (23). 2-Propanol was diffused to each solution to give red prismatic crystals of complex **5** or complex **6**. Elemental analysis: for complex **5** (dried under vacuum at 100°C) Δ-$[Co(Hbim)_3]\cdot H_2O$ ($C_{18}H_{17}N_{12}OCo$), calculated values were C, 51.77%; H, 4.10%; N, 40.25%; values found were C, 51.56%; H, 4.02%; N, 40.15%; IR (KBr) 2824 cm^{-1} [*br*, ν (NH)]; 1898 cm^{-1} [*br*, 2γ (NH)]. Elemental analysis: complex **6** (dried under vacuum at 100°C) λ-$[Co(Hbim)_3]\cdot H_2O$ ($C_{18}H_{17}N_{12}OCo$), calculated values were C, 51.77%; H, 4.10%; N, 40.25%; values found were C, 51.61%; H, 4.30%; N, 40.16%; IR (KBr) 2824 cm^{-1} [*br*, ν (NH)]; 1898 cm^{-1} [*br*, 2γ (NH)].

Crystal Structure Data for Complexes 2–6. Crystal data for complex **2**: $[Ni(Hbim)_2(^tBupy)_2]$ ($C_{30}H_{36}N_{10}Ni$), *triclinic*, space group *P*-1 (No. 2) with a = 10.395 (8) Å, b = 11.117 (6) Å, c = 8.425 (4) Å, α = 106.84 (5)°, β = 106.97 (5)°, γ = 104.33 (6)°, V = 830 (1) $Å^3$, Z = 1, ρ_{calcd} = 1.190 gcm^{-3}, F (000) = 314, T = 23°C, μ(MoKα) = 6.18 cm^{-1}, 215 parameters, R_1 = 0.089, R_w = 0.119, and GOF = 1.55 for all 1,314 data [I >4σ (I)]; values of minimum and maximum residual electron density 1.13 and −0.54 $eÅ^3$, 3,827 reflections were collected by Lp, and Ψ scan absorption correction was applied. Crystal data for complex **3**: $\{[Ni(Hbim)_2(bpy)]\}_2$ ($C_{44}H_{36}N_{20}Ni_2$); *orthorhombic*, space group *P*bca (No. 61) with a = 33.248 (6) Å, b = 16.832 (5) Å, c = 16.279 (4) Å, V = 9110 (6) $Å^3$, Z = 8, ρ_{calcd} = 1.403 gcm^{-3}, F (000) = 3968, T = 23°C, μ(MoKα) = 8.84 cm^{-1}, 740 parameters; R_1 = 0.042, R_w = 0.033, and GOF = 1.51 for all 3,727 data [I >3σ (I)]; values of minimum and maximum residual electron density 0.22 and −0.17 $eÅ^3$, 11,611 reflections were collected by Lp, and Ψ scan absorption correction was applied. Crystal data for complex **4**: $\{[Ru(Hbim)_3]\}_2$ ($C_{36}H_{30}N_{24}Ru_2$), *monoclinic*, space group $P2_1$ (No. 4) with a = 12.2426 (8) Å, b = 12.643 (1) Å, c = 13.2066 (6) Å, β = 92.738 (4)°, V = 2041.8 (2) $Å^3$, Z = 2, ρ_{calcd} = 1.628 gcm^{-3}, F (000) = 1004, T = 23°C, μ(CuKα) = 65.12 cm^{-1}, 560 parameters; R_1 = 0.042, R_w = 0.067, and GOF = 1.75 for all 2,776 data [I >3σ (I)]; values of minimum and maximum residual electron density 0.72 and −1.46 $eÅ^3$, 3,194 reflections were collected by Lp, and Ψ scan absorption correction was applied. Crystal data for complex **5:** $\{Δ\text{-}[Co(Hbim)_3]\}_2\cdot 3(2\text{-}PrOH)\cdot 2H_2O$ ($C_{45}H_{54}N_{24}O_5Co_2$), *orthorhombic*, space group $P2_12_12_1$ (No. 19) with a = 13.917 (4) Å, b = 31.216 (8) Å, c = 12.721 (5) Å, V = 5526 (2) $Å^3$, Z = 4, ρ_{calcd} = 1.362 gcm^{-3}, F (000) = 2360, T = −123°C, μ(CuKα) = 52.54 cm^{-1}; 686 parameters, R_1 = 0.044, R_w = 0.051, and GOF = 1.25 for all 2,913 data [I >3σ (I)]; values of minimum and maximum residual electron density 0.38 and −0.31 $eÅ^3$, 4,528 reflections were collected by Lp, and Ψ scan absorption correction was applied. Crystal data for complex **6:** $\{λ\text{-}[Co(Hbim)_3]\}_2\cdot 3(2\text{-}PrOH)\cdot 2H_2O$

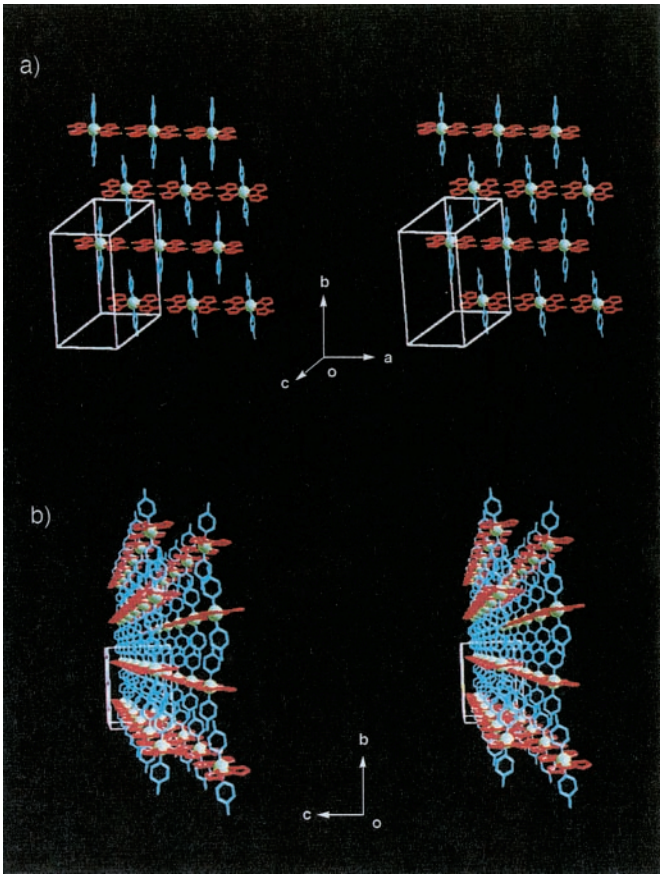

Fig. 2. Arrangement of one-dimensional linear chains in crystal formed by **2** (stereoviews). Three CH_3 groups containing ^{t}Bupy are omitted for clarity. (*a*) One-dimensional linear chains link along the *a* axis and pile along the *b* axis. $Hbim^{-1}$, red; Ni^{2+}, green; and ^{t}Bupy, blue. (*b*) A perspective stereoview of linear chains, as viewed along the *a* axis.

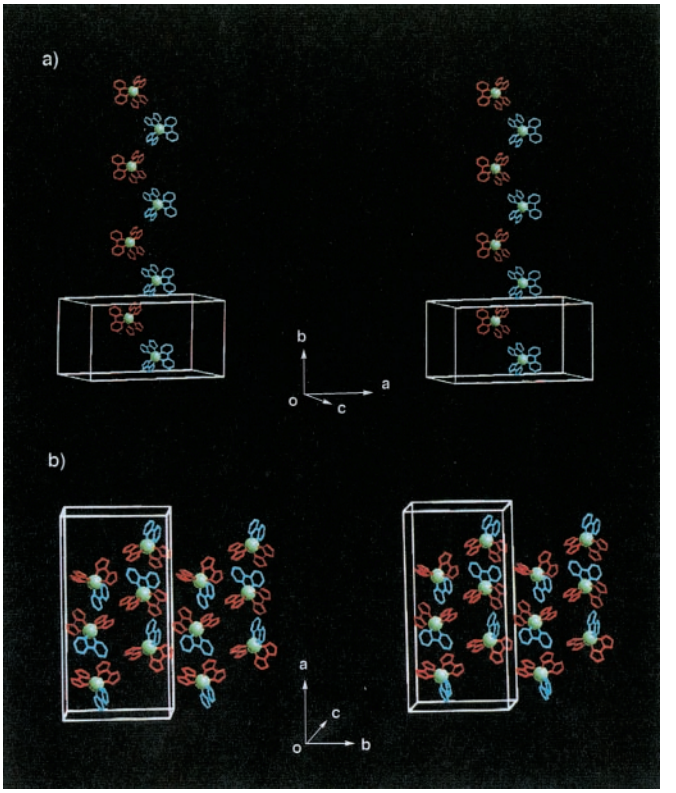

Fig. 3. Arrangement of one-dimensional zigzag ribbons in crystal formed by **3** (stereoviews). (*a*) A zigzag ribbon structure is formed by alternate linkage between different optical isomers of Δ (red) and λ (blue) types along the *b* axis. (*b*) Stacking of the zigzag ribbons along the *a* axis. $Hbim^{-1}$, red; Ni^{2+}, green; and bpy, blue.

($C_{45}H_{54}N_{24}O_5Co_2$), *orthorhombic*, space group $P2_12_12_1$ (No. 19) with $a = 13.90$ (3) Å, $b = 31.2$ (1) Å, $c = 12.71$ (1) Å, $V = 5516$ (19) Å^3, $Z = 4$, $\rho_{calcd} = 1.359$ gcm^{-3}, F (000) = 2360, $T = -123$°C, μ(CuKα) = 52.63 cm^{-1}; 686 parameters, $R_1 = 0.049$, $R_w = 0.068$, and GOF = 1.76 for all 3,327 data [I $>3\sigma$ (I)]; values of minimum and maximum residual electron density were 0.55 and -0.44 eÅ^3, 4,214 reflections were collected by Lp, and Ψ scan absorption correction was applied. A Rigaku AFC7R diffractometer (Rigaku, Tokyo) was used for all crystals; computing structure solution, SIR92 (24) for crystal complexes **2** and **5**; SHELXS-86 (25) for crystal complexes **3**, **4**, and **6**; computing structure refinement, DIRDIF94 (26) for all crystals; reflections for all crystals were refined based on F_o by full-matrix least squares. Crystallographic data (excluding structure factors) for the structures reported in this paper have been deposited with the Cambridge Crystallographic Data Center as CSD reference nos. 174718 (**2**), 174719 (**3**), 174720 (**4**), 174721 (**5**), and 174927 (**6**).

Results and Discussion

Classification of multidimensional superstructures has already been performed in organic compounds assembled by intermolecular H-bonding of carboxylic acid derivatives (27), as well as in coordination polymers by bridging ligands such as oxalate (28–31). Carboxylic acid H-bonding and oxalate-coordination polymer have been rationally synthesized in a linear chain, a zigzag ribbon, a honeycomb sheet, and other three-dimensional superstructures. These superstructures afford the classification of the multiaggregation compounds that consist of only H-bonds or coordination bonds. Here, we have established a new categorical classification of the superstructures generated by simultaneous use of both complementary intermolecular H-bondings and stable coordination bondings, as shown in Fig. 1.

The H-bonded dimer unit through the $Hbim^{-1}$ ligands has been assembled securely and strongly by using neutral complexes containing $Hbim^{-1}$ (Scheme 1). For example, the previously reported neutral [Cu^{II}(Hbim)(SalenNMe$_2$)] (**1**) is formed by an H-bonded dimer of the type A. In contrast, the positively charged [Cu^{II}(Hbim)(tacn)]$^+$ formed an intermolecular H-bonding interaction with ClO_4^- counter anion in preference to self-complementary NH···N H-bonding interaction between $Hbim^{-1}$ ligands (32). This result suggests that the counter ions, in particular, the anions with strong H-bonding ability in the ionic complexes, interrupt the formation of the dimer unit. Although counter cations like alkylammonium ions in the crystal with the anionic complex [$Ni(Hbim)_3]^{-1}$ affect the superstructures, they do not perturb the complementary H-bondings. Thus, these facts indicate that there is no chance of interruption of self-complementary ligand–ligand interactions because of sterically demanding bulky cations and the preferential H-bonding between $Hbim^{-1}$ ligands of anion complexes. From this point, to develop the effective self-organization of superstructures, neutral complexes rather than charged ones should be used.

Fig. 2 shows a superstructure with one-dimensional (1-D) linear chains of the type B constructed by neutral [$Ni^{II}(Hbim)_2(^tBupy)_2$] (**2**) with a *trans* configuration. The blue single crystals of **2** are obtained from a basic methanol solution by simple one-pot self-organization with Ni (II) ions, $Hbim^{-1}$ and ^{t}Bupy. The chain in the crystal along the *a* axis is composed

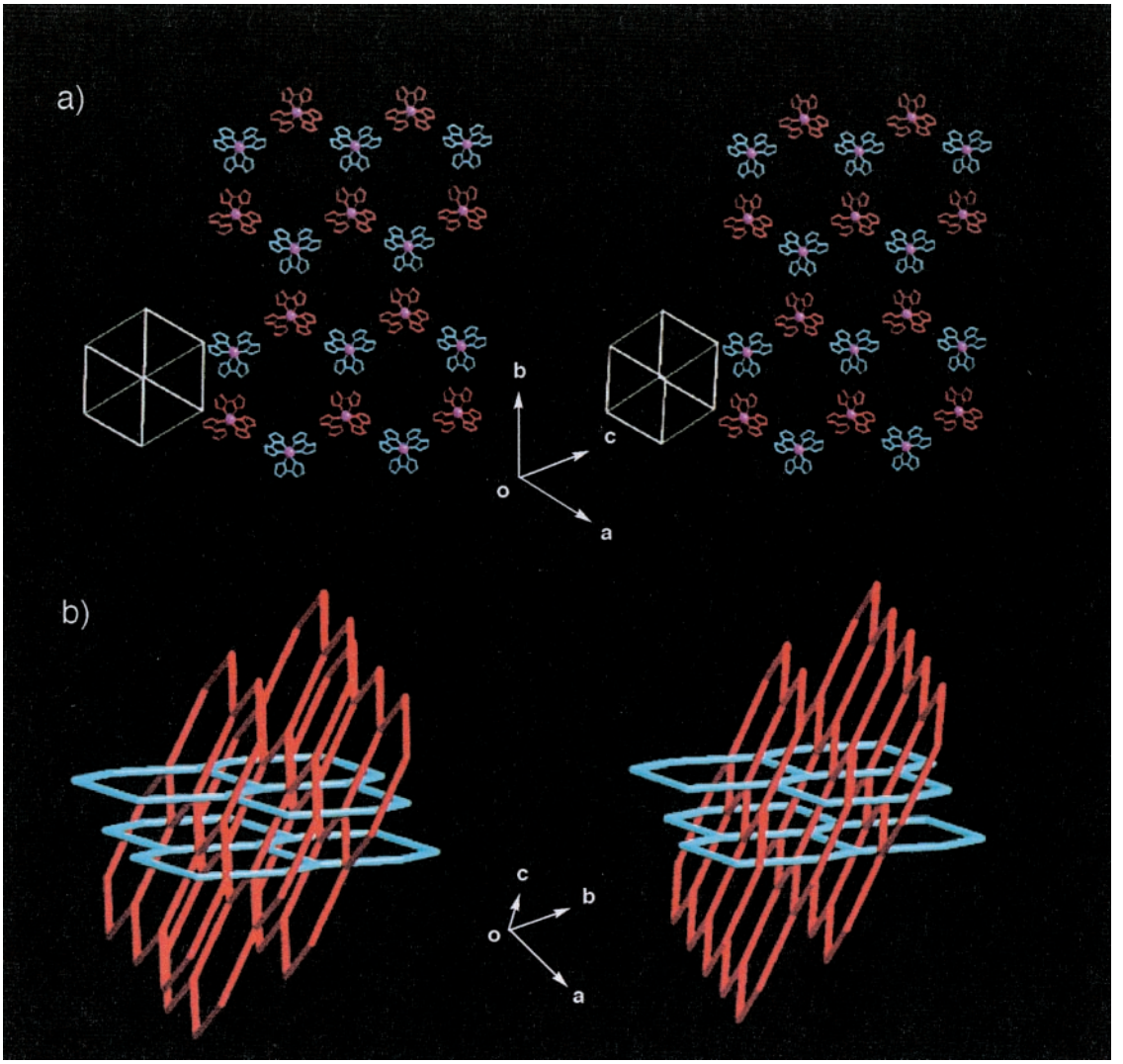

Fig. 4. Arrangement of two-dimensional honeycomb sheets in crystal formed by **4** (stereoviews). (*a*) A two-dimensional honeycomb sheet is formed by alternate linkage between different optical isomers of Δ (blue) and λ (red) types (Ru^{3+} ion is shown in magenta sphere). The sheet is constructed by complete hydrogen bonds on three $Hbim^{-1}$ sites of **4**. (*b*) Schematic drawing of the polycatenate network for the crystal of **4**. The straight lines represent the distance between Ru (III) ions in two $[Ru(Hbim)_3]$ building blocks connected by hydrogen bonds. Double-interlocking interpenetrations with the polycatenate structure are formed by two sets of stacked honeycomb sheets (red and blue lines) that are nearly perpendicular to each other in three-dimensionality.

of infinite links of intermolecular H-bonds of two $Hbim^{-1}$ ligands, located in equatorial positions on the distorted octahedron (the range of NH···N distances: 2.80 Å ~ 2.82 Å). The two axial positions are occupied by two monodentate ^{t}Bupy ligands. Each chain is piled along the *b* axis to form stacking sheets in the *ac* plane while fitting each ^{t}Bu group into the space between the chains. On the other hand, formation of the 1-D linear chains can be altered to that of 1-D zigzag-ribbons by changing the direction of intermolecular H-bonding sites in the building blocks. Fig. 3 shows the zigzag ribbon of the type C constructed by $[Ni^{II}(Hbim)_2(bpy)]$ (**3**) with the bpy ligand. The pale orange crystals of **3** are obtained by the same synthetic method of **2** except that the bidentate bpy was used instead of ^{t}Bupy. The zigzag ribbon consists of 1-D ordered arrays along the *b* axis formed by alternative H-bondings between different optical isomers of Δ and λ of **3**. Two $Hbim^{-1}$ ligands of **3** are used to form the H-bonded zigzag-ribbon networks, but a coordinated bpy does not participate in the formation of the networks (the range of NH···N distances: 2.78 Å ~ 2.83 Å). Each bpy residue on the zigzag ribbon is aligned standing alternately parallel to each other and perpendicular to the 1-D main chains. Thus, we have demonstrated that we can control linear vs. zigzag 1-D networks by using monodentate and bidentate ligands, respectively.

As shown in Fig. 4*a*, a neutral racemic complex of $[Ru^{III}(Hbim)_3]$ (**4**) with D_3 symmetry forms a two-dimensional honeycomb sheet of the type D with (6,3) nets. Compound **4** is prepared from the precursor complex $[Ru^{II}(H_2bim)_3]^{2+}$, and the desired dark blue single crystals are crystallized from a methanol solution. All of the three $Hbim^{-1}$ sites of **4** form the complementary intermolecular H-bonds completely. The honeycomb sheet self-organized by **4** is constructed by using alternative H-bondings between optical isomers of Δ and λ types of **4** (the range of NH···N distances; 2.79 Å ~ 2.80 Å). Each sheet forms an infinite number of identical sheets and passes each hexagonal cavity created by six **4** units through the two interpenetrating rods of the other two sheets at an inclination of ≈70° to give a three-dimensional (3-D) polycatenate structure with a double interlocking interpenetration (Fig. 4*b*). The two chiral building blocks of Δ-$[Co^{III}(Hbim)_3]$ (**5**) and λ-$[Co^{III}(Hbim)_3]$ (**6**) form

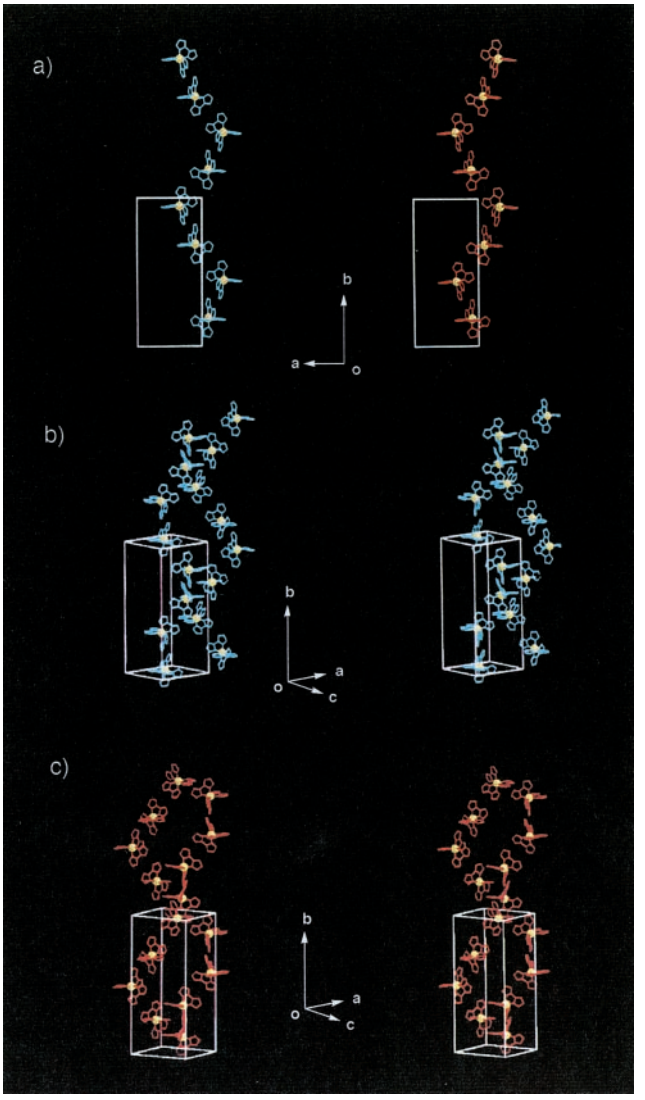

Fig. 5. Arrangement of helical chains in crystal formed by **5** or **6** (Co^{3+} ion is shown in yellow sphere). (*a*) View of each helical chain is represented by the left-handed helix formed by Δ-isomers of **5** in blue (the left-side view) or the right-handed one by λ-isomers of **6** in red (the right-side view) along the *c* axis. (*b*) A stereoview of two left-handed single helices by Δ-isomers of **5** (blue). Two single helices do not intersect each other and do not form a double helix. (*c*) A stereoview of two right-handed single helices by λ-isomers of **6** (red).

1-D helical chains of the type E (Fig. 5) with a left-handed and a right-handed orientation, respectively. The red single crystals of **5** and **6** are crystallized from 2-propanol by the deprotonation reaction of the optically resolved Δ− and λ-$[Co^{III}(Hbim)_3](NO_3)_3$ precursor complexes. Each 1-D helical chain is constructed by employing intermolecular H-bonds between the same optical isomers that use two of three $Hbim^{-1}$ sites in **5** or **6**. Both helical chains form 4_1 single strands, which have a pitch of ≈ 33.4 Å, similar to that of the B-DNA double strand. Another residual $Hbim^{-1}$ site of **5** or **6** is blocked by H-bonds with 2-propanol of crystallization, without using the helical chain construction.

In the case of a superstructure that uses all of three sites, a three dimensional chiral network with larger porous spaces formed by 8_7 cavities of (10,3)-*a* nets would be expected to be constructed as that found in the crystal with $[Ni(Hbim)_3]^{-1}$ building blocks, which has the structure reinforced by a 2-fold interpenetration and a stable double-helical structures (33). In contrast, the crystal of **5** or **6** does not have any larger porous networks. It has not been obvious to date why large cavities are not constructed by (10,3)-*a* single networks, although two factors, solvent effect and the strength of the H-bonds formed, are anticipated. Here, the two superstructures of a honeycomb sheet and a helical strand built from Tris-2,2′-biimidazolate complexes with D_3 symmetry can be individually prepared by using a racemic compound and an optically resolved one, respectively.

In summary, we demonstrated the practical structures of A ~ E in Fig. 1 based on the relationships between specified molecular arrays and molecular building blocks and identified the four types of new superstructures B ~ E by x-ray analysis. The knowledge from structural data should help provide the preprogramming of new superstructures built from the "neutral" $Hbim^{-1}$ complexes. Thus, we found that the neutral complexes with some $Hbim^{-1}$ ligands can control the preprogramming superstructures in multidimensionality by using configurations around the coordination sphere, because there is no chance of interruption of self-complementary ligand–ligand interactions caused by sterically demanding bulky cations and the preferential H-bonding between $Hbim^{-1}$ ligands of anion complexes.

Crystal engineering techniques that make use of those functionalized molecular building blocks will be employed in future studies for the creation of new solid-state materials. Thus, the building blocks in Fig. 1 would produce the functionalized preprogramming superstructures by introducing additive ligands with physical properties such as magnetic and photoactive ones to other coordination sites on the arrays of A, B, C, and E. Further attempts to develop functional solid-state materials with these techniques should be undertaken.

We thank the Analytical Center of Osaka City University for use of a four-circle single-crystal x-ray diffractometer and elemental analyses. This work was supported by a Grant-in-Aid for Scientific Research (nos. 13440201 and 10146103) on Priority Areas from the Ministry of Education, Science and Culture, Japan.

1. Batten, S. R. & Robson, R. (1998) *Angew. Chem. Int. Ed. Engl.* **37,** 1460–1494.
2. Zaworotko, M. J. (2001) *Chem. Commun.*, 1–9.
3. Vaidhyanathan, R., Natarajan, S. & Rao, C. N. (2001) *J. Chem. Soc. Dalton Trans.,* 699–706.
4. Kitagawa, S. & Kondo, M. (1998) *Bull. Chem. Soc. Jpn.* **71,** 1739–1753.
5. Holman, K. T., Pivovar, A. M., Swift, J. A. & Ward, M. D. (2001) *Acc. Chem. Res.* **34,** 107–118.
6. Sherrington, D. C. & Taskinen, K. A. (2001) *Chem. Soc. Rev.* **30,** 83–93.
7. Desiraju, G. R. (1995) *Angew. Chem. Int. Ed. Engl.* **34,** 2311–2327.
8. Desiraju, G. R. (2000) *J. Chem. Soc. Dalton Trans.*, 3745–3751.
9. Oda, R., Huc, I., Schmutz, M., Candau, S. J. & MacKlntosh, F. C. (1999) *Nature (London)* **399,** 566–599.
10. Cai, C., Müller, B., Weckesser, J., Barth, J. V., Tao, Y., Bösch, M. M., Kündig, A., Bosshard, C., Biaggio, I. & Günter, P. (1999) *Adv. Mater.* **11,** 750–754.
11. Höger, S., Bonrad, K., Mourran, A., Beginn, U. & Möller, M. (2001) *J. Am. Chem. Soc.* **123,** 5651–5659.
12. Fujita, M., Umemoto, K., Yoshizawa, M., Fujita, N., Kusukawa, T. & Biradha, K. (2001) *Chem. Commun*., 509–518.
13. Joachim, C., Gimzewski, J. K. & Aviram, A. (2000) *Nature (London)* **408,** 541–548.
14. Burrows, A. D., Chan, C.-W., Chowdhry, M. M., McGrady, J. E. & Mingos, D. M. P. (1995) *Chem. Soc. Rev.* **138,** 329–339.
15. Mitsumi, M., Toyoda, J. & Nakasuji, K. (1995) *Inorg. Chem.* **34,** 3367–3370.
16. Wilton-Ely, J. D. E. T., Schier, A., Mitzel, N. W. & Schmidbaur, H. (2001) *J. Chem. Soc. Dalton Trans.*, 1058–1062.
17. Yang, G., Zhu, H.-G., Ling, B.-H. & Chen, X.-M. (2001) *J. Chem. Soc. Dalton Trans.*, 580–585.
18. MacDonald, J. C., Dorrestein, P. C., Pilly, M. M., Foote, M. M., Lundburg, J. L., Henning, R. W., Schuitz, A. J. & Manson, J. L. (2000) *J. Am. Chem. Soc.* **122,** 11692–11702.
19. Beatty, A. M. (2001) *Cryst. Eng. Comm.* **51,** htpp://www.rsc.org/is/journals/current/crystengcomm/cechighlights.htm.

20. Tadokoro, M., Toyoda, J., Isobe, K., Itoh, T., Miyazaki, A., Enoki, T. & Nakasuji, K. (1995) *Chem. Lett.*, 613–614.
21. Tadokoro, M., Isobe, K., Uekusa, H., Ohashi, Y., Toyoda, J., Tashiro, K. & Nakasuji, K. (1999) *Angew. Chem. Int. Ed. Engl.* **38,** 95–98.
22. Rillema, P., Sahai, R., Matthews, P., Edwards, A. K. & Shaver, R. J. (1990) *Inorg. Chem.* **29,** 167–175.
23. Kanno, H., Manriki, S., Yamazaki, E., Utsuno, S. & Fujita, J. (1996) *Bull. Chem. Soc. Jpn.* **69,** 1981–1986.
24. Altomare, A., Burla, M. C., Camalli, M., Cascarano, M., Giacovazzo, C., Guagliardi, A. & Polidori, G. (1994) *J. Appl. Cryst.* **27,** 435.
25. Sheldrick, G. M. (1985) in *Crystallographic Computing***,** eds. Sheldrick, G. M., Krüger, C. & Smits, J. M. M. (Oxford Univ. Press), Vol. 3, pp. 175–189.
26. Beurskens, P. T., Admiraal, G., Beurskens, G. Bosman, W. P., de Gelder, R., Iarael, R. & Smits, J. M. M. (1994) *The DIRDIF-94 Program Systems* (Univ. of Nijmegen, Nijmegen, The Netherlands).
27. Desiraju, G. R. (2001) *Nature (London)* **412,** 397–400.
28. Coronado, E., Galán-Mascarós, J. R., Gomez-García, C. J. & Laukhin, V. (2000) *Nature (London)* **408,** 447–450.
29. Bénard, S., Yu, P., Audiére, J. P., Riviére, E., Clément, R., Guilhem, J., Tchertanov, L. & Nakatani, K. (2000) *J. Am. Chem. Soc.* **122,** 9444–9454.
30. Andrés, R., Brissard, M., Gruselle, M., Train, C., Vaissermann, J., Malezieux, B., Jamet, J.-P. & Verdaguer, M. (2001) *Inorg. Chem.* **40,** 4633–4640.
31. Decurtins, S., Ferlay, S., Pellax, R., Gross, M., Veciana, J. & Schmalle, H. (1999) in *Supramolecular Engineering of Synthetic Metallic Materials-Conductors and Magnets*, eds. Veciana, J., Rovira, C. & Amabilino, J. D. (Kluwer, Dordrecht, The Netherlands), pp. 175–196.
32. Tadokoro, M. & Nakasuji, K. (2000) *Coord. Chem. Rev.* **198,** 205–218.
33. Tadokoro, M., Shiomi, T., Isobe, K. & Nakasuji, K. (2001) *Inorg. Chem.* **40,** 5476–5478.